Eur J Nucl Med Mol Imaging (2010) 37:310–318
DOI 10.1007/s00259-009-1270-2

ORIGINAL ARTICLE

Potential impact of ^{68}Ga-DOTATOC PET/CT on stereotactic radiotherapy planning of meningiomas

Fonyuy Nyuyki · Michail Plotkin · Reinhold Graf · Roger Michel · Ingo Steffen · Timm Denecke · Lilli Geworski · Daniel Fahdt · Winfried Brenner · Reinhard Wurm

Received: 24 June 2009 / Accepted: 24 August 2009 / Published online: 18 September 2009

Abstract
Purpose Since meningiomas show a high expression of somatostatin receptor subtype 2, PET with ^{68}Ga-DOTATOC was proposed as an additional imaging modality beside CT and MRI for planning radiotherapy. We investigated the input of ^{68}Ga-DOTATOC-PET/CT on the definition of the "gross tumour volume" (GTV) in meningiomas, in order to assess the potential value of this method.

Methods Prior to radiotherapy, 42 patients with meningiomas (26 f, 16 m, mean age 55) underwent MRI and ^{68}Ga-DOTATOC-PET/CT examinations. History: operated n=24, radiotherapy n=1, operation and radiotherapy n=8, no treatment n=9. PET/CT and MRI data were co-registered using a BrainLAB workstation. For comparison, the GTV was defined first under consideration of CT and MRI data, then using PET data.

Results 3/42 patients were excluded from the analysis (two with negative PET results, one with an extensive tumour, not precisely delineable by MRI or PET/CT). The average $GTV_{CT/MRI}$ was 22(±19)cm³; GTV_{PET} was 23(±20)cm³. Additional GTV, obtained as a result of PET was 9(±10) cm³ and was observed in patients with osseous infiltration. In some pre-treated patients there were intratumoural areas (as identified in CT/MRI) without SR-expression (7(±11)cm³). Common GTV as obtained by both CT/MRI and PET was 15(±14)cm³. The mean bi-directional difference between the $GTV_{CT/MRI}$ and GTV_{PET} accounted to 16(±15)cm³ (93%, $p<$ 0.001). In a subgroup of seven patients with multiple meningiomas, PET showed a total of 19 lesions; nine of them were not recognizable by CT or MRI.

Conclusion ^{68}Ga-DOTATOC-PET enables delineation of SR-positive meningiomas and delivers additional information to both CT and MRI regarding the planning of stereotactic radiotherapy. The acquisition on a PET/CT scanner helps to estimate the relation of PET findings to anatomical structures and is especially useful for detection of osseous infiltration. ^{68}Ga-DOTATOC-PET also allows detection of additional lesions in patients with multiple meningiomas.

Keywords Meningioma · Somatostatin receptor · ^{68}Ga-DOTATOC · PET/CT · Target volume definition · Stereotactic radiotherapy

Fonyuy Nyuyki and Michail Plotkin contributed equally to this work.

F. Nyuyki · M. Plotkin (✉) · R. Michel · I. Steffen · L. Geworski · D. Fahdt · W. Brenner
Department for Nuclear Medicine,
Charité-Universitätsmedizin Berlin,
Charitéplatz 1,
10117 Berlin, Germany
e-mail: michail.plotkin@charite.de

T. Denecke
Department for Radiology, Campus Virchow,
Charité-Universitätsmedizin Berlin,
Berlin, Germany

R. Graf · R. Wurm
Department for Radiation Therapy, Campus Virchow,
Charité-Universitätsmedizin Berlin,
Berlin, Germany

L. Geworski
Department for Radiation Safety and Medical Physics,
Medizinische Hochschule Hannover,
Hannover, Germany

R. Wurm
Department for Radiation Therapy and Radiooncology,
Klinikum Frankfurt (Oder),
Frankfurt, Germany

Introduction

Meningiomas are mesodermal tumours originating in the arachnoid membrane and situated in the skull or spinal canal. With a yearly incidence of approximately 2.5–6 / 100,000 they constitute 13–26% of primary intracranial tumours [1, 2]. Even with apparent total removal, the recurrence rate varies from 9–19% at 10 years and up to 44% in the case of subtotal resection [2]. Because of the high rate of recurrence, a complete surgical resection is generally the treatment of choice, but is not always possible, especially when the tumour is located in the vicinity of critical intracranial structures like nerves or blood vessels impairing accessibility, or, for tumours located at the skull base, with possible infiltration of osseous structures. Radiotherapy offers a valuable therapeutic option and finds routine application in the therapy of anaplastic, atypical, malignant meningiomas, inoperable and residual tumours, recurrent meningiomas as well as in the therapy of meningiomatosis. In lesions smaller than 4 cm in diameter, a stereotactic radiotherapy is particularly helpful. An accurate delineation of the tumour from its surrounding structures is a premise for successful stereotactic radiotherapy.

Cerebral magnetic resonance imaging (MRI) and computer tomography (CT) are standard modalities for the planning of stereotactic radiotherapy. It has been shown that CT and MRI complement each other in the diagnosis of meningiomas [3]. CT has proven to be more effective than MRI in diagnosing bone infiltrations at the anterior region of the skull base [4, 5]. MRI has a higher soft-tissue contrast and allows much better differentiation between gray and white brain substance. Moreover, the meningeal structures can be visualised by MRI and the meningiomas can be easily detected with the use of intravenous contrast media [6, 7]. However, MRI is of limited specificity when distinguishing between tumour residues/recurrences and post-therapeutic changes such as scarring of the meningeal layers and tumour.

Receptor imaging offers an interesting additional tool for imaging of meningiomas. Meningiomas show a high expression of several receptors, among these, somatostatin receptor subtype 2 (SSTR 2) [8, 9]. The SSRT ligand [^{111}In]-DTPA-D-Phe^{1}-octreotide (^{111}In-octreotide) was shown to be valuable for differentiating meningiomas from other intracranial or intraspinal tumours like neurinomas, neurofibromas, and for post-surgical control and diagnosis of re-growth [10]. Because of a poor resolution of single photon emission computed tomography (SPECT), meningiomas with a diameter of less than 2.7 cm or a volume smaller than 10 ml cannot be detected [11]. Recently, another somatostatin analogue 1,4,7,10-tetraazacyclododecane-N,N′,N″,N‴-tetraacetic-acid-D-Phe1-Tyr3-octreotide (DOTATOC) capable of being labelled with the positron emitter ^{68}Ga (half-life, 68 min), was developed. ^{68}Ga-DOTATOC is a positron emission tomography (PET) tracer and shows an up to a nine-fold higher affinity to SSTR 2, as compared to ^{111}In-DTPA-octreotide [12].

In the present study we performed PET/CT using ^{68}Ga-DOTATOC in a group of 42 patients with meningiomas and retrospectively investigated the potential influence of PET on the definition of GTV, as compared to CT (as a part of PET/CT) and MRI. The purpose of the study was to assess the potential value of ^{68}Ga-DOTATOC PET/CT for planning stereotactic radiation therapy.

Material and methods

Patients

Enrolled in this study were 42 consecutive patients with known meningiomas (26 females; 16 males; age 21 to 73 years; mean age 55), who were referred for stereotactic radiation therapy to our centre between August 2006 and February 2008 (Table 1). In 33/42 patients who were pre-treated by surgery and/or radiation therapy (surgery n=24; radiation therapy n=1, both surgery and radiation therapy n=8), a recurrent/residual tumour was suspected based on MRI. Nine patients had no prior treatment. Since magnetic resonance imaging (MRI) was one of the imaging modalities to be compared with PET, patients who could not be examined with MRI (for example patients with metal implants) or patients not eligible for a PET examination (for example pregnant women) were not enrolled in the study. All patients were investigated by ^{68}Ga-DOTATOC PET/CT prior to radiation therapy.

The study was based on the Declaration of Helsinki and the principles of ‘good clinical practice’. The protocol was approved by the ethics committee of our institution. Written informed consent was obtained from all patients before enrolment into the study.

Methods

MR imaging

MRI of the skull was performed using a head coil in a 1.5 T scanner (1.5 T Signa, General Electric, Milwaukee, USA, or 1.5 T Philips Gyroscan ACS NT, Philips, Best, The Netherlands). T2-weighted spin-echo sequences (TR 2,500 ms/TE 80 ms; Matrix 256×256; one acquisition, 5-mm slice thickness) as well as T1-weighted spin-echo sequences (TR 700 ms/TE 15 ms; Matrix 512×512; one acquisition; 4–5 mm slice thickness) without and at least in two different dimensions after intravenous application of

Gadolinium-DTPA (Magnevist, Schering AG, Berlin) at a dosage of 0.1 mmol/kg of body weight were obtained.

PET/CT imaging

PET data were obtained in three-dimensional mode using a hybrid PET/CT system (Biograph 16 Siemens; Erlangen; Germany). ^{68}Ga was obtained from a ^{68}Ge/^{68}Ga radionuclide generator (Eckert & Ziegler, Berlin, Germany). For the synthesis of ^{68}Ga-DOTATOC, the method previously described by Zhernosekov et al. was used [13]. Labelling yields of >95% were achieved. The radiochemical purity was >99%. ^{68}Ga-DOTATOC was applied intravenously followed by a tracer uptake phase of 60 min as recommended by Henze et al. [14]. The applied dose of ^{68}Ga-DOTATOC was between 70 and 120 MBq. The patient was positioned in a dedicated positioning device for the head with an additional cushion and bandages for fixation. An unenhanced CT scan (detector collimation, 16×1.5 mm; tube current, 100 mA; tube voltage, 120 kV; gantry rotation time 0.8 s) covering the entire head was performed for attenuation correction. PET was acquired in a single bed position with a 16-cm axial FOV from the base of the skull to the vertex over 20 min. PET emission data were reconstructed iteratively (OSEM algorithm) using a 128×128 matrix.

Image fusion and data analysis

MRI and PET/CT data were transferred to a computer that supports a commercially available software package for radiation therapy planning (Brain SCAN 5.1, BrainLAB AG) and fused automatically using a mutual information algorithm. A detailed description of the method for image fusion was previously published by Grosu et al. who equally tested the validity of the software [15]. The analysis of the data and the delineation of the tumour margins were performed manually by an experienced radiation therapist and nuclear medicine physician.

We followed the definition of the gross tumour volume (GTV) recommended by report No. 50 (1993) of the international commission on radiation units and measurements(ICRU) and later on modified report No. 62 (1999) of the same commission [16, 17]. Hereby, the GTV is considered as the tumour volume detectable with diagnostic or operative methods. For the delineation of the "composite volume" ($GTV_{CT/MRI}$), data of both MRI and CT were considered: CT in bone and soft-tissue windowing as well as T1-weighted, fat-saturated MRI with and without gadolinium enhancement. The "composite volume" ($GTV_{CT/MRI}$) was therefore the volume that enclosed the tumour tissue, detectable by CT and/or MRI. In a separate step, the target volume was delineated using ^{68}Ga-DOTATOC-PET (GTV_{PET}). The volume GTV_{PET} was defined manually under consideration of areas with high ^{68}Ga-DOTATOC accumulation, following the method published by Astner et al. [18]. The threshold of PET windowing was adapted in regions where the tumour bordered to anatomical structures or normal brain tissue, which could be easily outlined in fused MR/PET images. Further, the GTV_{PET} and $GTV_{CT/MRI}$ were compared using fused PET/CT and MR images. GTV was defined enclosing all tumour areas visualized in all the three imaging modalities, i.e., CT, MRI and ^{68}Ga-DOTATOC-PET ($GTV_{CT/MRI/PET}$). We calculated the additional tumour volume with high receptor expression, shown by ^{68}Ga-DOTATOC-PET $\left(GTV_{PET}plus = GTV_{CT/MRI/PET} - GTV_{CT/MRI}\right)$, as well as volume of areas, which were not recognizable in PET, but detectable by CT and/or MRI $\left(GTV_{CT/MRI}plus = GTV_{CT/MRI/PET} - GTV_{PET}\right)$. Moreover, we calculated the bi-directional difference between the $GTV_{CT/MRI}$ and GTV_{PET}. The additional information, caused by the inclusion of PET in the radiation therapy planning was noted (e.g., invasion or infiltration of critical structures like the sinuses by the tumour, infiltration of osseous structures as well as detection of additional lesions).

Statistics

Statistical analysis was performed using R (Version 2.8.1; The R Foundation for Statistical Computing). Continuous data were described with mean (± standard deviation) and median (interquartile range [25th/75th percentiles]). Due to the small sample sizes, non-parametric distribution of data was assumed. Volumetric results of the PET, CT, and MRI in the same patient group were tested by the Wilcoxon test, whereas the Mann-Whitney-U-test was used for comparisons between the subgroups of pretreated and untreated patients.

Results

The determination of GTV was possible in MRI and/or CT in 41 out of 42 studied patients. Forty patients out of 42 showed areas with a high ^{68}Ga-DOTATOC uptake. Two patients (Nos. 39 and 40, Table 1), both with pre-treated tumours (surgery), were excluded from the study because the ^{68}Ga-DOTATOC-PET showed no SR-positive tumour in the Gd-enhancing lesions detected in post-surgical MRI. Another patient (No. 17) with an extensive tumour was excluded from the analysis, because the GTV could neither be precisely delineated by MRI nor by PET/CT. Thus, the final analysis was based on the comparison of 39 patients with the GTV definable in all modalities (MRI, CT, and PET).

The $GTV_{CT/MRI}$ equalled GTV_{PET} in 11/39 patients (28%). Consideration of ^{68}Ga-DOTATOC-PET led to a

Table 1 Patient history and volumetric results of CT/MRI and PET imaging

Patient no.	Sex	WHO Classification	Age	Location	Previous therapy	GTV $_{CT/MRI}$ (cm^3)	GTV $_{PET}$(cm^3)	GTV $_{PET}$ plus (cm^3)	GTV$_{CT/MRI}$ plus (cm^3)	Common GTV(cm^3)	Change in GTV by PET (cm^3)
1	F	WHO III	56	R sphenoid bone	Surg	18	18	4	4	14	8
2	M	WHO I	56	R cerebellopontine angle	Surg	18	11	0	7	11	7
3	F	WHO I, II	62	L falx	Surg, Rad	53	51	11	13	40	24
4	M	WHO III	58	L falx, L parieto-occipital convexity	Surg, Rad	18	9	1	9	9	10
5	M		63	L SB, multiple lesions	Surg	7	32	25	0	7	25
6	F		58	R medial sphenoid	None	11	12	2	1	10	3
7	F		60	SB, multiple lesions	Surg	25	24	4	4	20	8
8	F		60	Multiple lesions	Surg	67	55	5	17	50	22
9	F	WHO I	53	L SB	Surg	16	26	21	11	5	32
10	M	WHO I	69	L SB	Surg	19	6	3	16	31	19
11	F		67	R SB	None	1	4	3	0	1	3
12	M		67	L SB	None	36	24	2	14	22	16
13	M	WHO III	49	L frontal, L occipital convexity	Surg, Rad	76	19	4	61	15	65
14	M	WHO II	58	L occipital convexity	Surg	25	2	0	23	2	23
15	M	WHO III	71	L paracentral, L parietal convexity	Surg, Rad	13	35	26	4	9	30
16	F		46	L sphenoid bone, orbita infiltration	Surg	12	14	2	0	12	2
17[a]	F	WHO III	48	Massive expansion in several locations	Surg	NA	NA	NA	NA	NA	NA
18	F		48	L SB	None	4	6	2	0	4	2
19	F	WHO I	64	L sphenoid	None	4	7	5	3	2	8
20	M		71	L sphenoid bone, L frontal convexity	None	6	6	5	5	1	10
21	F		57	L petrous bone	Surg, Rad	8	12	4	0	8	4
22	F		65	R SB	Surg, Rad	54	58	11	7	47	18
23	M		50	L SB	None	15	12	3	6	9	9
24	F	WHO I	46	R SB	Surg	30	38	17	8	21	25
25	M		73	R SB	Surg	59	62	17	14	45	31
26	F	WHO III	54	Brain stem	Surg, Rad	1	1	1	1	1	2
27	F		53	R SB	None	32	26	22	28	4	50
28	M	WHO II	25	L SB	Surg	30	34	17	14	17	31
29	F		52	L SB	Surg	15	16	4	3	12	7
30	F	WHO I	50	R SB	Surg	29	47	18	0	29	18
31	M		31	R SB	Surg	11	14	6	3	8	9

32	F		52	Orbital cavity, N. opticus, L sphenoid wing	Surg	8	15	7	0	8	7
33	F		49	L SB	Rad	24	37	14	2	23	16
34	F	WHO I	48	L SB	Surg	39	90	51	0	39	51
35	M	WHO II	66	L SB, L orbita infiltration	Surg, Rad	29	27	2	3	26	5
36	M		21	R SB	Surg	3	6	4	2	2	6
37	F		63	R SB, R lateral orbita, R falx,	None	14	16	5	2	11	7
38	F		36	L SB	Surg	12	12	2	2	10	4
39[a]	F		51	L falx	Surg	NA	NA	NA	NA	NA	NA
40[a]	M	WHO II	55	L frontal convexity	Surg	NA	NA	NA	NA	NA	NA
41	F		55	R SB	Surg	21	26	6	1	20	7
42	F	WHO II	54	R frontobasal convexity	Surg	4	4	2	2	2	4
Mean			55			22	23	9	7	15	16
SD			11			19	20	10	11	14	15
Median						18	16	4	3	10	9

CT Computed tomography; *F* Female; *M* Male; *L*Left; *R*Right; *GTV* Gross tumour volume; *MRI* Magnetic resonance imaging; *PET* Positron emission tomography; *Rad* Radiation therapy; *SB* Skull base; *Surg* Surgery; *NA* Not available; *WHO* World Health Organization; GTV $_{PET}$ plus: Additional GTV as shown by PET, GTV $_{CT/MRI}$ plus: Additional GTV as shown by CT/MRI

[a] Patients Nos. 17, 39, and 40 were excluded from the final analysis

modification of GTV in 28/39 studied patients. $GTV_{CT/MRI}$ was larger than GTV_{PET} in 9/39 patients (23%) and smaller than GTV_{PET} in 19 patients (49%) (see example presented in Fig. 1). Interestingly, in all 28 patients, the differences in GTV_{PET} and $GTV_{CT/MRI}$ were bi-directional (both ^{68}Ga-DOTATOC-accumulating, CT/MRI-negative and non ^{68}Ga-DOTATOC-accumulating, CT/MRI-positive areas in the same patient). The mean $GTV_{CT/MRI}$ encompassing the volumes defined under consideration of CT and MRI was 22(±19)cm^3. The mean GTV_{PET} was 23(±20)cm^3 and showed no significant difference to $GTV_{CT/MRI}$ (p= 0.199). The implementation of ^{68}Ga-DOTATOC-PET data led to a mean increase of the final GTV by 9(±10)cm^3, as compared to volumes defined with CT and MRI only. On the other side, there were also areas categorized in CT or MRI as tumourous which did not show any SR expression (Fig. 2). Such areas without ^{68}Ga-DOTATOC accumulation had an average volume of 7(±11)cm^3. The intersection of $GTV_{CT/MRI}$ and GTV_{PET} averaged 15(±14)cm^3. The mean bi-directional difference between the $GTV_{CT/MRI}$ and GTV_{PET} was 16(±15)cm^3, which corresponds to a mean alteration of $GTV_{CT/MRI}$ of 93(±77)% (p<0.001). If looking at the subgroups of pretreated and untreated patients separately, the mean bi-directional difference between the $GTV_{CT/MRI}$ and GTV_{PET} was 87(±73)% in pretreated patients (n=30) and 113(±92)% in untreated patients (n= 9). A comparison of the amplitude of these bi-directional changes between both groups delivered no significant difference (p=0.589).

In nine patients, the $GTV_{CT/MRI}$ was larger than GTV_{PET}. Remarkably, six out of these nine patients had undergone previous treatment. On the other hand, GTV_{PET} was larger than $GTV_{CT/MRI}$ in 19 patients. ^{68}Ga-DOTATOC-PET/CT revealed an infiltration of the skull base in 29/39 patients. In eight out of these 29 patients, ^{68}Ga-DOTATOC-PET showed an infiltration of osseous structures, which was not detectable by CT (Fig. 1). An infiltration of the venous sinus, which was hardly (equivocal findings) detectable in MRI, was suggested by ^{68}Ga-DOTATOC-PET in five patients (Fig. 2). A high uptake of ^{68}Ga-DOTATOC was found in the pituitary glands of all the patients, hampering the PET-based demarcation of tumours in some cases.

In the subgroup of seven patients with multiple meningiomas, we performed an additional analysis on a lesional basis. ^{68}Ga-DOTATOC-PET demonstrated a total of 19 lesions in this subgroup, nine of which were not detectable by CT or by MRI (Fig. 3).

Discussion

This simulation study evaluated the potential role of ^{68}Ga-DOTATOC PET/CT in the radiation planning of meningiomas. If considering the PET data, the mean bi-directional percentage of GTV alteration (as compared to the composite volume) amounted to 93%. The GTV was modified based on ^{68}Ga-DOTATOC-PET data in 28/39 patients with positive PET scans (72%). In nine of the patients, the GTV_{PET} was smaller than the $GTV_{CT/MRI}$. Six of these nine patients have initially been pre-treated probably presenting areas with therapy-induced changes (post-radiation necrosis, scars) which in Gd-enhanced MRI are difficult to differentiate from viable tumour. On the other hand, GTV_{PET} was larger than the composite volume ($GTV_{CT/MRI}$) in 19 cases, 17 of which were skull base meningiomas. This observation confirms an earlier study revealing ^{68}Ga-DOTATOC-PET as being particularly valuable in providing additional information with regard to the extent of tumour infiltration into osseous structures at the skull base [14]. Moreover, an infiltration of the venous sinuses was detected with the help of ^{68}Ga-DOTATOC PET in five patients which was judged equivocal on MRI because of physiological gadolinium enhancement in the sinuses. Constrictively, it should be noted that in our study the 1.5 Tesla scanner was

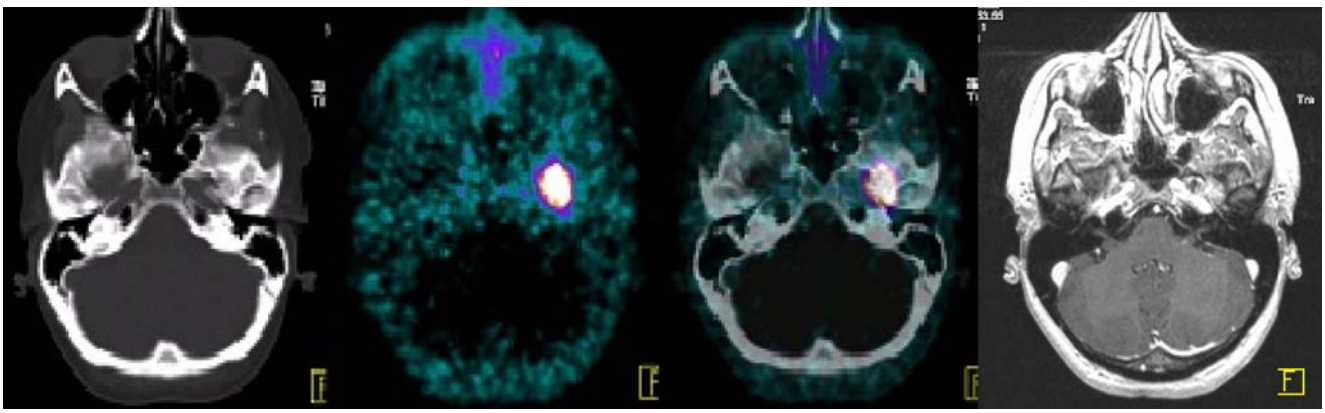

Fig. 1 A 36-year-old female patient (pat. No. 38) with a meningioma located at the base of the skull (left sphenoid bone): ^{68}Ga-DOTATOC-PET allows markedly better tumour delineation than CT and MRI

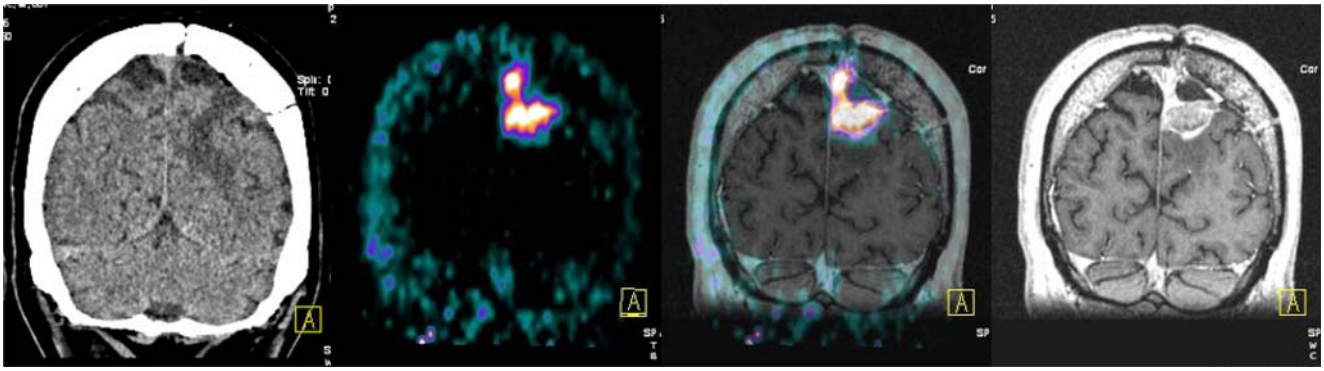

Fig. 2 A 58-year-old male patient (pat. No. 4) with relapse of an anaplastic meningioma (WHO III) in the left parieto-occipital convexity at left falx: Image fusion of ^{68}Ga-DOTATOC-PET and Gd-enhanced MRI demonstrates an infiltration of the superior sinus sagittalis, which is not clearly differentiated from a physiological Gd-enhancement in the sinus on MRI

used for MR imaging. The 3.0 Tesla MRI allows performing a high-spatial resolution 3D cerebral contrast-enhanced MR venography, which could have some advantages for detection of venous sinus invasion by meningiomas [19].

The results of the present PET/CT study confirm data published by Milker-Zabel et al., whereby in 19 out of 26 patients (73%), the planning target volume was significantly modified by the use of fused ^{68}Ga-DOTATOC-PET, CT, and MRI [20]. The high sensitivity and specificity of PET in the diagnosis of meningiomas can only be useful if a reliable topographic correlation/mapping with anatomical landmarks are available. In contrast to previous studies [14, 20, 21], we used a hybrid PET/CT system that allows a simultaneous acquisition of precisely co-registered PET and CT scans and facilitates implementation of ^{68}Ga-DOTATOC-PET data in radiation therapy planning. Since MRI compared to CT has some advantages in the diagnosis of meningiomas, an additional fusion of the MRI and PET/CT data offers additional clinically valuable information, as shown by our simulation study.

PET with radio-labelled amino acids represents an alternative approach for metabolic imaging of meningiomas [18, 22–26]. Astner et al. [18] showed that ^{11}C-methionine PET can influence the radiotherapy planning in the majority (29/32) of patients with base skull meningiomas resulting in both increase, as well as in a decrease of GTV. Interestingly, in the study by Astner et al. the MET-PET was able to detect small tumour portions that were not identified by CT or MRI. The intensity of the ^{11}C-MET uptake has been shown to correlate with the Ki67 index. Unfortunately, the ^{11}C-methionine is of limited availability due to the short physical half-life (20 min) of the isotope ^{11}C and can be used only in a few PET centres equipped with a cyclotron. Rutten et al. reported the use of a fluorinated amino acid tracer, ^{18}F-TYR for GTV estimation in 11 patients with skull base meningiomas (n=13 lesions) and found that the ^{18}F-TYR uptake extended beyond the MRI lesion in 38% of the tumours, and were smaller in 8% of the tumours [23]. Another ^{18}F-labelled synthetic tyrosine derivate, ^{18}F-FET, which was thoroughly validated in the diagnosis of gliomas [27–29], might be useful in the diagnostic evaluation of meningiomas. In contrast to the ^{11}C-methionine, the ^{18}F-FET does not accumulate in the pituitary gland and might therefore have potential advantages over the ^{68}Ga-DOTATOC for detecting intrasellar invasion of meningiomas. Indeed, in some patients in our study, the meningiomas with close proximity to the sella turcica could not be reliably differentiated from the adjacent pituitary gland,

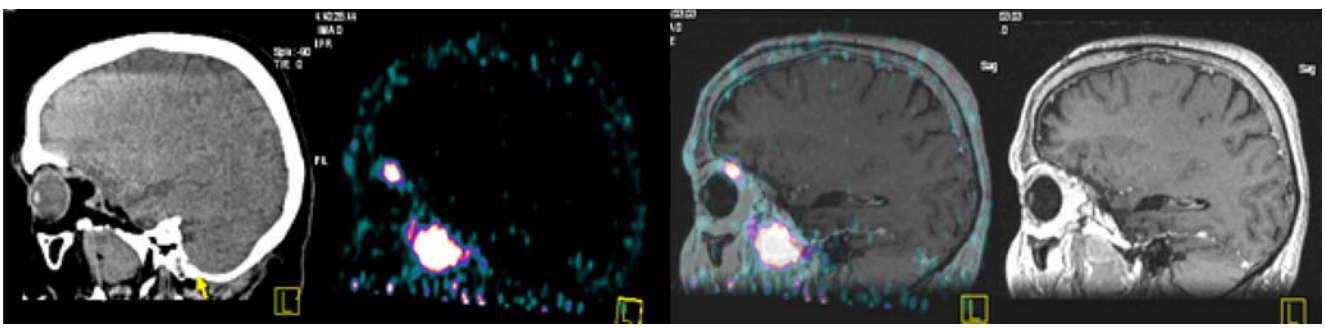

Fig. 3 A 63-year-old male patient (pat. No. 5) with multifocal meningioma. MRI and PET/CT showed a recurrent tumour at the base of the skull 2 years after the resection. ^{68}Ga-DOTATOC-PET showed an additional intra-orbital lesion that could not be detected with Gd-enhanced MRI

showing a physiologically high expression of somatostatin receptors. On the other hand, a high accumulation of ^{18}F-FET in sinuses could hamper the detection of sinus infiltration, which can be easily visualised using ^{68}Ga-DOTATOC. Up to now, no clinical studies have compared ^{18}F-FET with ^{68}Ga-DOTATOC and no studies have investigated ^{18}F-FET uptake in meningiomas. This issue should be a matter of further comparative investigations.

Similar to many studies on target volume definition of meningiomas, the main limitation of our study, being a simulative study is the lack of histological verification. Thus, the reason for negative PET results in two patients (Nos. 39 and 40) cannot be estimated because of the lack of an in-depth verification. These patients (who both underwent radiation therapy) were excluded from the final analysis. On the other hand, false-positive findings cannot be totally excluded, but appear unlikely since the uptake of DOTATOC to SSTR is known to be highly specific. Before a definite recommendation for the adjustment of radiation therapy to GTV_{PET}, histological correlations of ^{68}Ga-DOTATOC uptake patterns in meningiomas has to be performed, this is a current project at our medical centre.

Conclusion

^{68}Ga-DOTATOC-PET enables a delineation of the SR-positive tumour volume of meningiomas, delivering valuable additional information on tumour size and extent to both CT and MRI. We conclude that ^{68}Ga-DOTATOC-PET represents a very promising imaging tool for planning stereotactic radiotherapy. The acquisition of ^{68}Ga-DOTATOC-PET data on a PET/CT scanner helps to estimate the relation of PET findings to anatomical structures and seems to be especially useful for detection of bone infiltrations. Moreover, ^{68}Ga-DOTATOC-PET seems useful in patients of multiple meningiomas presenting with a higher sensitivity of lesion detection than CT or MRI.

References

1. Preston-Martin S. Descriptive epidemiology of primary tumors of the brain, cranial nerves and cranial meninges in Los Angeles County. Neuroepidemiology. 1989;8:283–95.
2. Simpson D. The recurrence of intracranial meningiomas after surgical treatment. J Neurol Neurosurg Psychiatry. 1957;20:22–39.
3. Khoo VS, Adams EJ, Saran F, Bedford JL, Perks JR, Warrington AP, et al. A comparison of clinical target volumes determined by CT and MRI for the radiotherapy planning of base of skull meningiomas. Int J Radiat Oncol Biol Phys. 2000;46:1309–17.
4. Tomura N, Hirano H, Sashi R, Hashimoto M, Kato K, Takahashi S, et al. Comparison of MR imaging and CT in discriminating tumour infiltration of bone and bone marrow in the skull base. Comput Med Imaging Graph. 1998;22:41–51.
5. Paling MR, Black WC, Levine PA, Cantrell RW. Tumor invasion of the anterior skull base: a comparison of MR and CT studies. J Comput Assist Tomogr. 1987;11:824–30.
6. Weingarten K, Ernst RJ, Jahre C, Zimmerman RD. Detection of residual or recurrent meningioma after surgery: value of enhanced vs. unenhanced MR imaging. Am J Roentgenol. 1992;158:645–50.
7. Schörner W, Schubeus P, Henkes H, Lanksch W, Felix R. "Meningeal sign": a characteristic finding of meningiomas on contrast-enhanced MR images. Neuroradiology. 1990;32:90–3.
8. Dutour A, Kumar U, Panetta R, Ouafik L, Fina F, Sasi R, et al. Expression of somatostatin receptor subtypes in human brain tumors. Int J Cancer. 1998;76:620–7.
9. Schulz S, Pauli SU, Schulz S, Händel M, Dietzmann K, Firsching R, et al. Immunohistochemical determination of five somatostatin receptors in meningioma reveals frequent over expression of somatostatin receptor subtype sst2A. Clin Cancer Res. 2000;6:1865–74.
10. Schmidt M, Scheidhauer K, Luyken C, Voth E, Hildebrandt G, Klug N, et al. Somatostatin receptor imaging in intracranial tumours. Eur J Nucl Med. 1998;25:675–86.
11. Bohuslavizki KH, Brenner W, Braunsdorf WE, Behnke A, Tinnemeyer S, Hugo HH, et al. Somatostatin receptor scintigraphy in the differential diagnosis of meningioma. Nucl Med Commun. 1996;17:302–10.
12. Reubi JC, Schär JC, Waser B, Wenger S, Heppeler A, Schmitt JS, et al. Affinity profiles for human somatostatin receptor subtypes SST1-SST5 of somatostatin radiotracers selected for scintigraphic and radiotherapeutic use. Eur J Nucl Med. 2000;27:273–82.
13. Zhernosekov KP, Filosofov DV, Baum RP, Aschoff P, Bihl H, Razbash AA, et al. Processing of generator-produced ^{68}Ga for medical application. J Nucl Med. 2007;48:1741–8.
14. Henze M, Schuhmacher J, Hipp P, Kowalski J, Becker DW, Doll J, et al. PET imaging of somatostatin receptors using [^{68}GA] DOTA-D-Phe1-Tyr3-octreotide: first results in patients with meningiomas. J Nucl Med. 2001;42:1053–6.
15. Grosu AL, Lachner R, Wiedenmann N, Stärk S, Thamm R, Kneschaurek P, et al. Validation of a method for automatic image fusion (BrainLAB System) of CT data and 11C-methionine-PET data for stereotactic radiotherapy using a LINAC: first clinical experience. Int J Radiat Oncol Biol Phys. 2003;56:1450–63.
16. *ICRU Report 50*. Prescribing, recording and reporting photon beam therapy. Bethesda, MD: International Commission on Radiation Units and Measurements; 1993.
17. *ICRU Report 62*. Prescribing, recording and reporting photon beam therapy. Supplement to ICRU Report 50. Bethesda, MD: International Commission on Radiation Units and Measurements; 1999.
18. Astner ST, Dobrei-Ciuchendea M, Essler M, Bundschuh RA, Sai H, Schwaiger M, et al. Effect of ^{11}C-Methionine-Positron emission tomography on gross tumor volume delineation in stereotactic radiotherapy of skull base meningiomas. Int J Radiat Oncol Biol Phys. 2008;15:1161–7.
19. Nael K, Fenchel M, Salamon N, Duckwiler GR, Laub G, Finn JP, et al. Three-dimensional cerebral contrast-enhanced magnetic resonance venography at 3.0 Tesla: initial results using highly accelerated parallel acquisition. Invest Radiol. 2006;41(10):763–8.
20. Milker-Zabel S, Zabel-du Bois A, Henze M, Huber P, Schulz-Ertner D, Hoess A, et al. Improved target volume definition for fractionated stereotactic radiotherapy in patients with intracranial meningiomas by correlation of CT, MRI, and [^{68}Ga]-DOTATOC-PET. Int J Radiat Oncol Biol Phys. 2006;65:222–7.
21. Henze M, Dimitrakopoulou-Strauss A, Milker-Zabel S, Schuhmacher J, Strauss LG, Doll J, et al. Characterization of ^{68}Ga-DOTA-D-Phe^{1}-

Tyr^3-octreotide kinetics in patients with meningiomas. J Nucl Med. 2005;46:763–9.
22. Grosu AL, Weber WA, Astner ST, Adam M, Krause BJ, Schwaiger M, et al. ^{11}C-methionine PET improves the target volume delineation of meningiomas treated with stereotactic fractionated radiotherapy. Int J Radiat Oncol Biol Phys. 2006;66:339–44.
23. Rutten I, Cabay JE, Withofs N, Lemaire C, Aerts J, Baart V, et al. PET/CT of skull base meningiomas using 2–18F-fluoro-L-tyrosine: initial report. J Nucl Med. 2007;48:720–5.
24. Iuchi T, Iwadate Y, Namba H, Osato K, Saeki N, Yamaura A, et al. Glucose and methionine uptake and proliferative activity in meningiomas. Neurol Res. 1999;21:640–4.
25. Nyberg G, Bergstrom M, Enblad P, Lilja A, Muhr C, Langstrom B. PET-methionine of skull base neuromas and meningiomas. Acta Otolaryngol. 1997;117:482–9.
26. Gudjonsson O, Blomquist E, Lilja A, Ericson H, Bergström M, Nyberg G. Evaluation of the effect of high-energy proton irradiation treatment on meningiomas by means of 11C-L-methionine PET. Eur J Nucl Med. 2000;27:1793–9.
27. Weber W, Wester HJ, Grosu AL, Herz M, Dzewas B, Feldmann HJ, et al. O-(2-[18F] fluoroethyl)-L-tyrosine and L-[methyl-11C] methionine uptake in brain tumours: initial results of a comparative study. Eur J Nucl Med. 2000;27:542–9.
28. Pauleit D, Floeth F, Hamacher K, et al. O-(2-[18F]fluoroethyl)-L-tyrosine PET combined with MRI improves the diagnostic assessment of cerebral gliomas. Brain. 2005;128: 678–87.
29. Stockhammer F, Plotkin M, Amthauer H, van Landeghem FK, Woiciechowsky C. Correlation of F-18-fluoro-ethyl-tyrosin uptake with vascular and cell density in non-contrast-enhancing gliomas. J Neuro Oncol. 2008;88:205–10.